

Peet Kask · Rolf Günther · Peter Axhausen

Statistical accuracy in fluorescence fluctuation experiments

Received: 13 February 1996 / Accepted: 20 September 1996

Abstract The mathematical expression of the signal to noise ratio in fluorescence fluctuation experiments is derived for arbitrary sample profiles and for any mechanism of translational motion, and experimentally verified. The signal to noise ratio depends on the mean count rate per particle per dwell time, the mean number of particles per sample volume, time characteristics of the correlation function, sample profile characteristics, and the data collection time. Statistical accuracy of the third order moment of fluorescence intensity fluctuations is also studied. The optimum concentration for the third order moment analysis is about one particle per sample volume.

Key words Fluorescence correlation spectroscopy · Fluorescence intensity fluctuations · Fluorescence intensity distribution analysis

1 Introduction

Fluorescence intensity fluctuations can be studied in different ways. Usually, the light intensity autocorrelation function $G(\tau) = \langle I(t) I(t+\tau) \rangle$ (I denoting fluorescence intensity) is calculated, yielding information about concentrations, intensities and dynamic properties of fluorescent particles. The corresponding field of research is called fluorescence correlation spectroscopy (FCS, Elson and Magde 1974). Sometimes, however, only the distribution of the photon count number is measured and the first two or three moments of light intensity, $\langle I \rangle$, $\langle I^2 \rangle$, and $\langle I^3 \rangle$, are calculated (Qian and Elson 1990a). The optical scheme of the experiment is identical in both cases: using a laser, a microscope, and a sensitive photon detector, movement of

a single molecule into and out of the beam focus can easily be detected (Rigler et al. 1993).

Fluorescence fluctuation studies is a field of science where optimization of experimental conditions and improvement of the design plays an unusually important role. One can find a number of published examples where hours of data collection time was needed in order to extract a useful signal from statistical noise.

In spite of the importance of the subject, there are very few papers dealing with matters of statistical accuracy in fluorescence fluctuation experiments. D. E. Koppel's fundamental paper (Koppel 1974) was published immediately after the first experiments (Magde et al. 1974) in which thousands of molecules were studied at a time. Correspondingly, Koppel's calculations assume relatively high concentration, $m \gg 1$ (with m being the mean number of fluorescent particles per sample volume). Under this condition, the signal to noise ratio of FCS experiments does not depend on particle concentration. Concerning the dependence of noise on count rate, Koppel distinguishes the "Poisson noise limit," corresponding to low count rate where the noise is determined by the quantum nature of light detection, from the "optimal high-counting-rate limit," where the noise is due solely to the stochastic nature of the movement of molecules. (We refer to these as "photon noise limit" and "molecular noise limit," respectively.)

H. Qian's paper (Qian 1990) is an extension of Koppel's earlier work. He considered the two-dimensional Gaussian sample profile instead of the uniform spot of Koppel's theory. Also, Qian's theory includes low concentration ranges ($m \ll 1$), where the signal to noise ratio is proportional to \sqrt{m} .

The goal of the present paper is to derive a quantitative expression for the signal to noise ratio in terms of measurable parameters for arbitrary sample profiles and for any mechanism of translational motion (e.g. diffusion, or flow). In particular, as an approximation of the epi-objective geometry of experiments, a sample profile which is Gaussian in two dimensions and Lorentzian in the third one will be studied.

P. Kask · R. Günther (✉) · P. Axhausen
EVOTEC BioSystems GmbH, Grandweg 64, D-22529 Hamburg,
Germany (Fax +49-40-5608 12 22; e-mail: guenther@evotec.de)

2 Theory

2.1 Basic assumptions and logic of the following calculations

In a number of aspects, the basic logical scheme of our study follows that of Qian's.

As usual, we assume that fluorescence is collected from a relatively small volume situated within a much larger volume of sample solution. This corresponds to the so-called open volume experiments.

In making our statistical accuracy calculations we shall express moments and correlation functions of fluorescence intensity based on the theoretical case of a single particle in a large volume inside which the small observation volume is defined.

We also follow our predecessors by studying an ideal solution of a single species. This means that all fluorescent particles are identical and their motion and fluorescence properties do not depend on the presence of other particles. Provided we have expressed moments and correlation functions of fluorescence intensity corresponding to a single particle, it is a purely technical exercise in statistics to express moments of fluorescence intensity and their variances for the case of a large number (M) of particles in the large volume.

As a final step, we shall calculate the statistical accuracy of the measured second order central moment of light intensity corresponding to the dwell time T and the data collection time NT . Since we use equivalent normalization procedures for moments and autocorrelation functions, the second order central moment of light intensity is equivalent to the amplitude of the time-dependent part of the autocorrelation function. More importantly, the estimate of the second order central moment of light intensity (as used in the moment analysis) is identical to the content of the 'zeroth channel' of the correlator (provided that the shot noise contribution is properly excluded in both cases). Therefore, the expression we derive for the signal to noise ratio of the estimate of the second order central moment of light intensity can also be used in correlation analysis.

2.2 Moments of fluorescence intensity corresponding to a single particle: characteristics of sample profile

As a model of experimental geometry, we assume the fluorescent particle to be situated randomly at any point in a relatively large volume V of radius R . We characterize the small volume from which fluorescence emission is collected by a radius parameter w (or a set of radius parameters corresponding to different dimensions, e.g. w_{xy} and w_z). More precisely than by the radius w , the sample is characterized by its profile function

$$S(\mathbf{r}) = I(\mathbf{r})/I_0, \quad (1)$$

where $I(\mathbf{r})$ is the fluorescence intensity (measured as the expected photon count rate), provided the particle is situ-

ated at the point \mathbf{r} , and I_0 is the maximum fluorescence intensity, usually corresponding to the centre of the sample ($\mathbf{r}=0$).

For the sake of simplicity, we now assume that the fluorescence intensity depends on the translational coordinate \mathbf{r} only (we ignore fluctuations corresponding to rotational motion or triplet trapping which usually occur on a faster time scale than translational motion through the sample volume). With this assumption, the k -th moment of the collected fluorescence intensity is expressed as

$$\varphi_k \equiv \langle I^k \rangle = \frac{1}{V} \int_{(V)} I^k(\mathbf{r}) d\mathbf{r} \quad (2)$$

$$= \frac{I_0^k}{V} \int_{(V)} S^k(\mathbf{r}) d\mathbf{r}. \quad (3)$$

The integrals $\int_{(V)} S^k(\mathbf{r}) d\mathbf{r}$ have the dimensions of volume; we shall denote them by v_k . From Eq. (3) we get

$$\varphi_k = I_0^k \frac{v_k}{V}. \quad (4)$$

Theoretical values of v_k corresponding to a number of alternative sample profile functions are shown in Table 1.

In real experiments, the set of v_k is not estimated. Instead, the concept of a single (apparent) sample volume v and the (apparent) count rate per particle q is used. In terms of the v_k 's, v can be expressed as (Qian and Elson 1990b)

$$v = \frac{v_1^2}{v_2}. \quad (5)$$

The (apparent) count rate per molecule is not exactly equal to the true count rate per molecule in the centre of the beam, I_0 , but equals

$$q = \frac{v_2}{v_1} I_0. \quad (6)$$

Note that for the Gaussian-Gaussian-Lorentzian sample profile, v is four times larger than v_1 and, correspondingly, q is four times lower than I_0 . It is essential that this fact be accounted for when planning experiments or interpreting results.

After the change of variables in accordance with Eqs. (5) and (6), Eq. (4) takes on the form

$$\varphi_k = \frac{q^k}{\gamma_k} \frac{v}{V}, \quad (7)$$

where we have denoted

$$\gamma_k = \frac{v_2^{k-1}}{v_1^{k-2} v_k}. \quad (8)$$

For any beam profile $\gamma_1 = \gamma_2 = 1$, and for the Gaussian-Gaussian-Lorentzian beam profile $\gamma_3 = 0.5$ and $\gamma_4 = 0.2$. The values of γ_3 and γ_4 can be experimentally determined for each set-up (Qian and Elson 1990b).

It is worth noting that Eq. (7) can be derived even if we disregard the assumption that fluorescence intensity is a

Table 1 Characteristics of seven alternative sample profiles

Sample profile name	Profile function	v_1	v_k/v_1				
			$k=2$	3	4	5	6
One-dimensional rectangular	1, if $x \leq w$ 0, if $x > w$	$2w$	1	1	1	1	1
One-dimensional Gaussian	e^{-2x^2/w^2}	$\sqrt{\frac{\pi}{2}} w$	$\frac{1}{\sqrt{2}}$	$\frac{1}{\sqrt{3}}$	$\frac{1}{2}$	$\frac{1}{\sqrt{5}}$	$\frac{1}{\sqrt{6}}$
One-dimensional Lorentzian	$\frac{w^2}{w^2 + x^2}$	πw	$\frac{1}{2}$	$\frac{3}{8}$	$\frac{5}{16}$	$\frac{35}{128}$	$\frac{63}{256}$
Two-dimensional disk	1, if $r \leq w$ 0, if $r > w$	πw^2	1	1	1	1	1
Two-dimensional Gaussian	e^{-2r^2/w^2}	$\frac{\pi w^2}{2}$	$\frac{1}{2}$	$\frac{1}{3}$	$\frac{1}{4}$	$\frac{1}{5}$	$\frac{1}{6}$
Three-dimensional Gaussian	e^{-2r^2/w^2}	$\left(\frac{\pi}{2}\right)^{3/2} w^3$	$\frac{1}{2\sqrt{2}}$	$\frac{1}{3\sqrt{3}}$	$\frac{1}{8}$	$\frac{1}{5\sqrt{5}}$	$\frac{1}{6\sqrt{6}}$
Gaussian-Gaussian-Lorentzian	$\frac{A^2}{A^2 + z^2} \times e^{-2(x^2+y^2)/w^2}$	$\frac{\pi^2 w^2 A}{2}$	$\frac{1}{4}$	$\frac{1}{8}$	$\frac{5}{64}$	$\frac{7}{128}$	$\frac{21}{512}$

function of the translational coordinates of the molecule only. In this case, however, Eq. (2) has to be modified, and, consequently, v_k 's and γ_k 's become more complicated to describe. Their values are influenced by contributions to fluorescence intensity fluctuations from rotational and electronic coordinates of the molecule. Note, however, that the rest of our calculations are not affected by the physical meaning of the variables in Eq. (7).

2.3 Correlation functions of fluorescence intensity corresponding to a single particle

So far, we have expressed moments of fluorescence intensity, $\langle I^k \rangle$, corresponding to a single particle and denoted them by φ_k . Below (when we calculate the variance of the experimental estimate of the second order moment of fluorescence intensity corresponding to many particles) we shall also need data regarding the autocorrelation functions of fluorescence intensity corresponding to a single particle, $\langle I^m(0) I^n(\tau) \rangle$, for $m, n \leq 2$. We denote them by $\varphi_{mn}(\tau)$. No assumption is made concerning the mechanism of translational motion, however, we just note again that at $\tau=0$ the correlation function equals the corresponding moment of light intensity. For $\tau \neq 0$, the correlation function usually decays monotonically in τ , with the time constant being characteristics for the translational process. For large values of τ it approaches zero because we let $V \rightarrow \infty$. Expressing $\varphi_{mn}(\tau)$ as a product of an amplitude φ_{m+n} and a shape function $g_{mn}(\tau)$, we get

$$\varphi_{mn}(\tau) = \varphi_{m+n} g_{mn}(\tau), \quad (9)$$

where

$$g_{mn}(0) = 1 \quad (10)$$

$$g_{mn}(\infty) = 0. \quad (11)$$

2.4 Moments of fluorescence intensity corresponding to M fluorescent particles

Now we assume that we have M independent and identical particles in the same large volume V where we previously had only one particle. Fluorescence intensity collected from the sample is simply a sum of contributions from each particle:

$$I = I_1 + I_2 + \dots + I_M \quad (12)$$

where I_1, I_2, \dots, I_M are contributions to fluorescence intensity from the first, the second, ..., and the M -th particle, respectively.

We can now proceed, making use of the assumption that particles are independent and identical. The first moment of I is expressed as

$$\langle I \rangle = \langle I_1 + I_2 + \dots + I_M \rangle = M \langle I_1 \rangle = M \varphi_1. \quad (13)$$

To express higher moments of I , we also make use of Eq. (12) and need only count the number of similar terms. We get

$$\begin{aligned} \langle I^2 \rangle &= \langle (I_1 + I_2 + \dots + I_M)^2 \rangle \\ &= M \langle I_1^2 \rangle + M(M-1) \langle I_1 I_2 \rangle \\ &= M \varphi_2 + M(M-1) \varphi_1^2. \end{aligned} \quad (14)$$

In our approach, M is a very large number and we can omit lower order terms of M , replacing $M(M-1)$ by M^2 . We get

$$\langle I^2 \rangle = M \varphi_2 + M^2 \varphi_1^2. \quad (15)$$

In a similar manner we get

$$\langle I^3 \rangle = M \varphi_3 + 3M^2 \varphi_2 \varphi_1 + M^3 \varphi_1^3, \quad (16)$$

$$\begin{aligned} \langle I^4 \rangle &= M \varphi_4 + 4M^2 \varphi_3 \varphi_1 + 3M^2 \varphi_2^2 \\ &\quad + 6M^3 \varphi_2 \varphi_1^2 + M^4 \varphi_1^4. \end{aligned} \quad (17)$$

2.5 Moments of photon count numbers corresponding to M fluorescent particles

In experiments, the light intensity is measured N times, counting the number of detected photons (we denote them by Z) in each of the N consecutive time intervals of duration T . Counting the number of photoelectron pulses is not a precise measurement of the classical light intensity I (which in our model is only a function of coordinates of the M molecules), but carries with it a random error due to the quantum nature of light and its detection. Therefore, the moments of photon count numbers Z are not correct estimates of the moments of I . Instead, factorial moments of Z serve that purpose (Saleh 1974). It is convenient to define a unit of fluorescence intensity as corresponding to one count per dwell time, then Saleh's statement is expressed as

$$\langle I \rangle = \langle Z \rangle \quad (18)$$

$$\langle I^2 \rangle = \langle Z(Z-1) \rangle \quad (19)$$

$$\langle I^3 \rangle = \langle Z(Z-1)(Z-2) \rangle \quad (20)$$

$$\langle I^4 \rangle = \langle Z(Z-1)(Z-2)(Z-3) \rangle, \quad (21)$$

which is equivalent to

$$\langle Z \rangle = \langle I \rangle \quad (22)$$

$$\langle Z^2 \rangle = \langle I^2 \rangle + \langle I \rangle \quad (23)$$

$$\langle Z^3 \rangle = \langle I^3 \rangle + 3\langle I^2 \rangle + \langle I \rangle \quad (24)$$

$$\langle Z^4 \rangle = \langle I^4 \rangle + 6\langle I^3 \rangle + 7\langle I^2 \rangle + \langle I \rangle. \quad (25)$$

Now we replace variables on the right side of Eqs. (22)–(25) by the corresponding expressions of Eqs. (15)–(17), and get

$$\langle Z \rangle = M\varphi_1 \quad (26)$$

$$\langle Z^2 \rangle = M(\varphi_2 + \varphi_1) + M^2\varphi_1^2 \quad (27)$$

$$\langle Z^3 \rangle = M(\varphi_3 + 3\varphi_2 + \varphi_1) + M^2\varphi_1(\varphi_2 + \varphi_1) + M^3\varphi_1^3 \quad (28)$$

$$\begin{aligned} \langle Z^4 \rangle = & M(\varphi_4 + 6\varphi_3 + 7\varphi_2 + \varphi_1) \\ & + M^2(4\varphi_3\varphi_1 + 3\varphi_2^2 + 18\varphi_2\varphi_1 + 7\varphi_1^2) \\ & + M^3(6\varphi_2\varphi_1^2 + 6\varphi_1^3) + M^4\varphi_1^4. \end{aligned} \quad (29)$$

2.6 Correlation functions of photon count numbers corresponding to M fluorescent particles

To express correlation functions of photon count numbers for non-zero delay times, we employ the same procedure as used to derive Eqs. (26)–(29). This is a straightforward, relatively simple mathematical exercise to do so; hence we present the results only:

$$\langle Z(0)Z(kT) \rangle = M\varphi_{11}(kT) + M^2\varphi_1^2 \quad (30)$$

$$\begin{aligned} \langle Z(0)Z^2(kT) \rangle = & M[\varphi_{12}(kT) + \varphi_{11}(kT)] \\ & + M^2\varphi_1(\varphi_2 + \varphi_1) \\ & + 2M^2\varphi_1\varphi_{11}(kT) + M^3\varphi_1^3 \end{aligned} \quad (31)$$

$$\begin{aligned} \langle Z^2(0)Z^2(kT) \rangle = & M[\varphi_{22}(kT) + 2\varphi_{12}(kT) + \varphi_{11}(kT)] \quad (32) \\ & + M^2[4\varphi_1(\varphi_{12}(kT) + \varphi_{11}(kT)) \\ & + (\varphi_2 + \varphi_1)^2 + 2\varphi_{11}^2(kT)] \\ & + M^3[2\varphi_1^2(\varphi_2 + \varphi_1) + 4\varphi_{11}(kT)\varphi_1^2] \\ & + M^4\varphi_1^4. \end{aligned}$$

2.7 Estimates of the second order central moment of fluorescence intensity

It is possible to estimate the second order autocorrelation function of fluorescence intensity fluctuations in a number of different ways. Koppel studied three alternative estimates. The best among them (corresponding to the smallest statistical error) is the following:

$$\hat{G}^{(2)}(kT) = \frac{1}{N} \sum_{i=1}^N Z_i Z_{i+k} - \frac{1}{N^2} \left(\sum_{i=1}^N Z_i \right)^2. \quad (33)$$

Subscript at Z is the number of the counting interval. The second term of Eq. (33) stands for subtracting the constant level of the first term. At the zero delay $k=0$, Eq. (33) needs slight modification; we must account for only cross-correlations between different photon pulses, subtracting the shot noise contribution:

$$\hat{G}_0^{(2)} = \frac{1}{N} \sum_{i=1}^N Z_i(Z_i-1) - \frac{1}{N^2} \left(\sum_{i=1}^N Z_i \right)^2. \quad (34)$$

Equation (34) is a mathematical expression of the estimate of the second central moment of light intensity, which is the equivalent of the amplitude of the correlation function of light intensity fluctuations. The assumption of Eqs. (33) and (34) is that the width of the dwell time is selected to be much shorter than the correlation time of fluorescence intensity fluctuations.

We shall calculate the expected value of $\hat{G}_0^{(2)}$ now.

$$\langle \hat{G}_0^{(2)} \rangle = \frac{1}{N} \sum_{i=1}^N \langle Z_i^2 \rangle - \frac{1}{N} \sum_{i=1}^N \langle Z_i \rangle - \frac{1}{N^2} \left\langle \sum_{i=1}^N Z_i \sum_{j=1}^N Z_j \right\rangle. \quad (35)$$

All N terms of $\sum_{i=1}^N \langle Z_i^2 \rangle$ are equivalent; so are all N terms of $\sum_{i=1}^N \langle Z_i \rangle$. However, there are N different ways how Z_i and Z_j can be combined. Most of them have relatively large values of $k=|i-j|$ for which $\langle Z_i Z_j \rangle \approx \langle Z \rangle^2$. In order to be precise, we do not replace $\langle Z_i Z_j \rangle$ by $\langle Z \rangle^2$ but also account deviations $\langle Z_i Z_j \rangle - \langle Z \rangle^2$. We get from Eq. (35)

$$\begin{aligned} \langle \hat{G}_0^{(2)} \rangle = & \langle Z^2 \rangle - \langle Z \rangle - \langle Z \rangle^2 - \frac{1}{N} (\langle Z^2 \rangle - \langle Z \rangle^2) \\ & - \frac{2}{N} \sum_{k=1}^{N-1} \frac{N-k}{N} (\langle Z(0)Z(kT) \rangle - \langle Z \rangle^2) \\ = & \frac{N-1}{N} (\langle Z^2 \rangle - \langle Z \rangle^2) - \langle Z \rangle \\ & - \frac{2}{N} \sum_{k=1}^{N-1} \frac{N-k}{N} (\langle Z(0)Z(kT) \rangle - \langle Z \rangle^2). \end{aligned} \quad (36)$$

The second central moment is actually equivalent to the expression $\langle Z^2 \rangle - \langle Z \rangle^2$. The right side of Eq. (36) is smaller than this, which means that our estimate is biased. The relative bias is small if N is sufficiently large. In fact, we can forget the bias, but the terms proportional to N^{-1} play a very important role when we calculate the variance of $\hat{G}_0^{(2)}$.

As a starting point in calculations of the variance, we take

$$\text{var}(\hat{G}_0^{(2)}) = \langle \hat{G}_0^{(2)2} \rangle - \langle \hat{G}_0^{(2)} \rangle^2. \quad (37)$$

We use expression (34) to replace $\hat{G}_0^{(2)}$ on the right side of Eq. (37). We implement the same mathematical technique again as when deriving Eq. (36). Unfortunately, the calculation is very tedious and we have to omit most of its details here. An important point (which can be used as a check against calculation errors) is that the terms independent of N compensate each other and cancel to zero. What remains non-zero are terms proportional to N^{-1} :

$$\begin{aligned} \text{var}(\hat{G}_0^{(2)}) &= \frac{1}{N} \times \left[\langle Z^4 \rangle - \langle Z^2 \rangle^2 \right. \\ &+ 2 \sum_{i=1}^{N-1} \frac{N-i}{N} (\langle Z^2(0) Z^2(iT) \rangle - \langle Z^2 \rangle^2) \\ &- 4 \langle Z \rangle (\langle Z^3 \rangle - \langle Z^2 \rangle \langle Z \rangle) \\ &- 8 \langle Z \rangle \sum_{i=1}^{N-1} \frac{N-i}{N} (\langle Z^2(0) Z(iT) \rangle - \langle Z^2 \rangle \langle Z \rangle) \\ &+ 4 \langle Z \rangle^2 (\langle Z^2 \rangle - \langle Z \rangle^2) \\ &+ 8 \langle Z \rangle^2 \sum_{i=1}^{N-1} \frac{N-i}{N} (\langle Z(0) Z(iT) \rangle - \langle Z \rangle^2) \\ &- 2 (\langle Z^3 \rangle - \langle Z^2 \rangle \langle Z \rangle) \\ &- 4 \sum_{i=1}^{N-1} \frac{N-i}{N} (\langle Z^2(0) Z(iT) \rangle - \langle Z^2 \rangle \langle Z \rangle) \\ &- 2 \langle Z \rangle (\langle Z^2 \rangle - \langle Z \rangle^2) \\ &- 4 \langle Z \rangle \sum_{i=1}^{N-1} \frac{N-i}{N} (\langle Z(0) Z(iT) \rangle - \langle Z \rangle^2) \\ &+ \langle Z^2 \rangle - \langle Z \rangle^2 \\ &\left. + 2 \sum_{i=1}^{N-1} \frac{N-i}{N} (\langle Z(0) Z(iT) \rangle - \langle Z \rangle^2) \right] \quad (38) \end{aligned}$$

Now we can apply Eqs. (26)–(32). The result is as follows:

$$\begin{aligned} \text{var}(\hat{G}_0^{(2)}) &= \frac{1}{N} \left[M \left(\varphi_4 + 2 \sum_{i=1}^{N-1} \frac{N-i}{N} \varphi_{22}(iT) + 4 \varphi_3 + 2 \varphi_2 \right) \right. \\ &\left. + M^2 \left(2 \varphi_2^2 + 4 \sum_{i=1}^{N-1} \frac{N-i}{N} \varphi_{11}^2(iT) + 4 \varphi_2 \varphi_1 + 2 \varphi_1^2 \right) \right]. \quad (39) \end{aligned}$$

Just as we applied Eqs. (26)–(32) to Eq. (38), we can apply them in the same manner to Eq. (36). Here we omit

terms proportional to N^{-1} . We get

$$\langle \hat{G}_0^{(2)} \rangle = M \varphi_2. \quad (40)$$

Now we make use of Eq. (4), applying it to both Eqs. (39) and (40). We let $M \rightarrow \infty$ and $V \rightarrow \infty$ but keep $Mv/V \equiv m$ constant, which is the mean number of particles per sample volume. From Eq. (40) we get

$$\begin{aligned} \langle \hat{G}_0^{(2)} \rangle &= M I_0^2 v_2 / V \\ &= m q^2 \end{aligned} \quad (41)$$

and from Eq. (39)

$$\begin{aligned} \text{var}(\hat{G}_0^{(2)}) &= m \left[\frac{q^4}{\gamma_4} (1 + 2 K_1) + 4 \frac{q^3}{\gamma_3} + 2 q^2 \right] \\ &+ m^2 [2 q^4 (1 + 2 K_1) + 4 q^3 + 2 q^2], \end{aligned} \quad (42)$$

where

$$K_1 = \sum_{i=1}^{N-1} \frac{N-i}{N} g_{22}(iT) \quad (43)$$

and

$$K_2 = \sum_{i=1}^{N-1} \frac{N-i}{N} g_{11}^2(iT). \quad (44)$$

To a crude approximation, the values of K_1 and K_2 can be calculated as integrals,

$$K_1 \approx \frac{1}{T} \int_0^\infty g_{22}(\tau) d\tau \equiv \frac{\tau_1}{T}, \quad (45)$$

$$K_2 \approx \frac{1}{T} \int_0^\infty g_{11}^2(\tau) d\tau \equiv \frac{\tau_2}{T}. \quad (46)$$

We shall use Eqs. (41) and (42) to express the signal to noise ratio. For applications, it is convenient to have expressed it through count rate per particle (Q) rather than through count number per particle and dwell time (q). Also, we prefer to use data collection time (U) rather than total number of time intervals (N). After the change of variables, the signal to noise ratio is expressed as

$$\frac{\langle \hat{G}_0^{(2)} \rangle}{\text{var}^{1/2}(\hat{G}_0^{(2)})} = \sqrt{\frac{U}{TR}}, \quad (47)$$

where R is an abbreviation of

$$\begin{aligned} R &= 2(1 + 2 K_2) + \frac{4}{QT} + \frac{2}{(QT)^2} \\ &+ \frac{1}{m} \left[\frac{1}{\gamma_4} (1 + 2 K_1) + \frac{4}{\gamma_3 QT} + \frac{2}{(QT)^2} \right]. \end{aligned} \quad (48)$$

Depending on values of m and QT , different terms on the right side of Eq. (48) dominate. In limit cases, the signal to noise ratio is expressed as

$$S/N = \sqrt{\frac{U}{2T(1 + 2 K_2)}} = \sqrt{\frac{U}{2\tau_2}}, \quad m \gg 1, \quad QT \gg 1, \quad (49)$$

$$S/N = Q \sqrt{\frac{UT}{2}}, \quad m \gg 1, \quad QT \ll 1, \quad (50)$$

$$S/N = \sqrt{\frac{U\gamma_4 m}{T(1+2K_1)}} = \sqrt{\frac{U\gamma_4 m}{\tau_1}}, \quad m \ll 1, \quad QT \gg 1, \quad (51)$$

$$S/N = Q \sqrt{\frac{UTm}{2}}, \quad m \ll 1, \quad QT \ll 1. \quad (52)$$

2.8 Interpretation of Eq. (42)

Above we have omitted lengthly details of the mathematics involved. Technically, the derivation of Eq. (42) is rather complicated. In fact, before solving the problem in its most complicated form, we studied a number of simpler models.

The simplest model studied includes the following additional assumptions: (1) the classical fluorescence intensity is measured exactly (without the photon noise); and (2) fluorescence intensities measured at different consecutive time steps are uncorrelated. Under these two assumptions the solution of the problem (corresponding to Eq. (39)) takes on a rather simple form:

$$\text{var}(\hat{G}_0^{(2)}) = \frac{1}{N} (M\varphi_4 + 2M^2\varphi_2^2). \quad (53)$$

A slightly more complicated model which uses assumption (2) but accounts for photon noise leads to

$$\text{var}(\hat{G}_0^{(2)}) = \frac{1}{N} [M(\varphi_4 + 4\varphi_3 + 2\varphi_2) + M^2(2\varphi_2^2 + 4\varphi_2\varphi_1 + 2\varphi_1^2)]. \quad (54)$$

However, if photon noise is not accounted for but time correlations are, then we arrive at

$$\text{var}(\hat{G}_0^{(2)}) = \frac{1}{N} \left[M \left(\varphi_4 + 2 \sum_{i=1}^{N-1} \frac{N-i}{N} \varphi_{22}(iT) \right) + M^2 \left(2\varphi_2^2 + 4 \sum_{i=1}^{N-1} \frac{N-i}{N} \varphi_{11}^2(iT) \right) \right]. \quad (55)$$

The most general model leads to Eq. (39) in which all terms appearing either in Eq. (53), (54), or (55) are present. This kind of dependence on the model gives us a good foundation for distinguishing between molecular and photon noise: all terms in Eq. (55) describe molecular noise, while the four terms in Eq. (54) which are absent in Eq. (55) describe photon noise. It is not surprising that at a high count rate $q \gg 1$, Eq. (39) yields Eq. (55), i.e. the terms corresponding to photon noise can be neglected.

2.9 Statistical accuracy of the estimate of the third order central moment of fluorescence intensity

The same two simple models which yield Eqs. (53) and (54) were used to study the statistical accuracy of the estimate of the third central moment of fluorescence intensity. The simpler model of the two correspondence to the estimate

$$\hat{G}_0^{(3)} = \frac{1}{N} \sum_i I_i^3 - \frac{3}{N^2} \sum_i I_i^2 \sum_j I_j + \frac{2}{N^3} \left(\sum_j I_j \right)^3 \quad (56)$$

and yields

$$\text{var}(\hat{G}_0^{(3)}) = \frac{1}{N} [M\varphi_6 + 9M^2(\varphi_4\varphi_2 + \varphi_3^2) + 6M^3\varphi_2^3], \quad (57)$$

while the model which also accounts for photon noise, but still assumes independent measurements, leads to

$$\text{var}(\hat{G}_0^{(3)}) = \frac{1}{N} [M(\varphi_6 + 9\varphi_5 + 18\varphi_4 + 18\varphi_3) + M^2(9\varphi_4\varphi_2 + 9\varphi_3^2 + 9\varphi_4\varphi_1 + 72\varphi_3\varphi_2 + 36\varphi_3\varphi_1 + 54\varphi_2^2 + 54\varphi_2\varphi_1) + M^3(6\varphi_2^3 + 18\varphi_2^2\varphi_1 + 18\varphi_1^3)]. \quad (58)$$

The most important character of $\hat{G}_0^{(3)}$ (compared to $\hat{G}_0^{(2)}$) is the existence of an optimum concentration for measurements. Indeed, while at high concentration values ($m \gg 1$), the signal to noise of $\hat{G}_0^{(2)}$ is independent of concentration, $\hat{G}_0^{(3)}$ can best be measured at an intermediate concentration range of about one particle per sample volume. At higher concentrations, the dominating term of the expression of $\text{var}(\hat{G}_0^{(3)})$ is proportional to m^3 while the value of $\hat{G}_0^{(3)}$ itself is only proportional to m .

3 Experimental test of Eq. (47)

3.1 Experimental procedures

We tested Eq. (47) by determining the experimental signal to noise ratio of $\hat{G}_0^{(2)}$ in studying rhodamine 6G solutions on a ConfoCor device (EVOTEC BioSystems and Carl Zeiss, Germany). The dye concentration was in the range of about 2×10^{-11} to 2×10^{-7} M (corresponding to about 0.04 to 400 dye molecules per sample volume) and the laser beam power was varied between 4 and 800 μ W (yielding about 1,400 to 160,000 counts per second and molecule). In order to determine the experimental variance of $\hat{G}_0^{(2)}$, we collected 20 distributions of the number of photon counts in 20 consecutive experiments of 2 s duration at a dwell time of $T = 50$ μ s. This procedure was repeated at each combination of values for m and Q .

For each measured distribution of the number of photon counts, $\hat{G}_0^{(2)}$ was calculated. At count rates exceeding 200 kHz we found it necessary to correct data for the dead time of the photon detector (30 ns). For dead time corrections we simply multiplied the calculated second factorial moment of the number of photon counts by a correction factor. The correction factor was kept constant for a given series of 20 measurements; its value was empirically selected to be consistent with correct values of m and Q (which could be determined at low count rates when dead time corrections are neglectable, or independently by FCS). Although the maximal shift of the value of the second factorial moment was only 0.28 percent, values of $\hat{G}_0^{(2)}$ were shifted by a factor of about two (which occurred at the highest concentration studied). In order to avoid significant errors due to dead time distortions, we did not use higher count rates than 2 MHz.

3.2 The results

Figure 1 presents data of the experimentally determined statistical accuracy (circles). In the upper graph, the signal to noise ratio (S/N) is plotted against concentration m . Data measured at two intensities of excitation (corresponding to 55 and 3.2 kHz per molecule) are presented. In the lower graph, the signal to noise ratio is plotted against the count rate per molecule. Data measured for two samples (corresponding to $m=0.15$ and $m=10.0$) are presented in this graph.

The theoretical curves of S/N corresponding to Eq. (47) are represented by smooth curves. Values of both m and Q were determined from the measured data and checked by FCS. The value of K_2 was calculated from the fit curve of the measured second order correlation function using Eq. (44) to be $K_2=3.14\pm 0.04$. (The characteristic time constant of the second order correlation function was $220\ \mu\text{s}$.) The value of K_1 was calculated using Eq. (43) assuming that $g_{22}(\tau)$ is of the same shape as $g_{11}(\tau)$ except having two times faster decay, which yielded $K_1=7.7$. We have experimentally determined $\gamma_3=0.53$ and $\gamma_4=0.23$ for our set-up.

4 Discussion

There were no free parameters when the theoretical curves of Fig. 1 were calculated. Therefore, the good quantitative agreement between the theory and experimental results is direct proof that Eq. (47) predicts accuracy of fluorescence fluctuation experiments.

In spite of its “awful” outlook, Eq. (47) (in complex with Eqs. (48), (43) and (44)) is a valuable formula for practical applications. Its strength is its universality: it can be applied at arbitrary sample profiles and at arbitrary shape of the correlation function. We can use it in ordinary FCS or in the scanning-FCS experiments, as well as in moment analysis of fluorescence intensity distribution. The formula is useful when optimizing conditions or designing new schemes of experiments.

It must be stressed that Eq. (47) expresses the signal to noise ratio of a particular estimate of the second order central moment of light intensity. It is not necessarily correct if a different definition of the signal was used. Also, our formula corresponds to statistical noise only: other possible sources of errors have not been accounted for. Most important, our definition of the signal to noise ratio measures the reproducibility of data, i.e. deviations from measurement to measurement, and not, for example, deviations of the measured correlation function from its fit curve.

As is illustrated by Fig. 1, both parameters m and Q should be kept sufficiently high in experiments whenever possible. What is meant by “sufficiently high” has to be specified in each particular case. The curves shown in Fig. 1 serve as an example where the mean count number $q=1$ (corresponding to $Q=20\ \text{kHz/molecule}$) is sufficiently high, while we still profit considerably from going

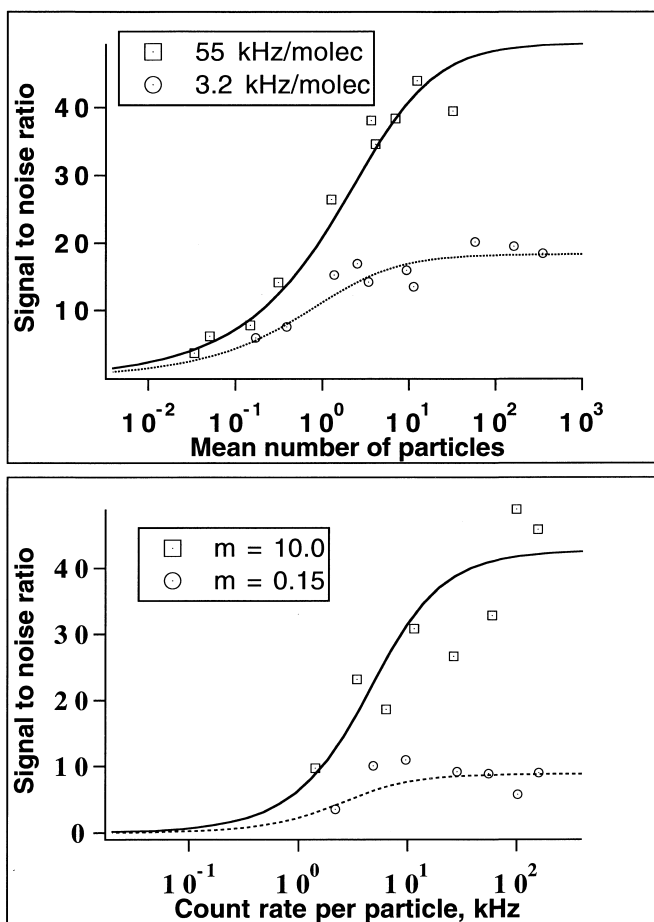


Fig. 1 Experimental test of Eq. (45): signal to noise ratio corresponding to the time window of $50\ \mu\text{s}$ and the measurement time of 2 s, on rhodamine 6G diffusion in water. Upper graph: measurements on different samples at two excitation intensities. Lower graph: measurements on two samples at different excitation intensities

up with the mean number of particles from its unit value $m=1$.

References

- Elson EL, Magde D (1974) Fluorescence correlation spectroscopy. I. Conceptual basis and theory. *Biopolymers* 13:1–27
- Koppel DE (1974) Statistical accuracy in fluorescence correlation spectroscopy. *Phys Rev A* 10:1938–1945
- Magde D, Elson EL, Webb WW (1974) Fluorescence correlation spectroscopy. II. An experimental realization. *Biopolymers* 13:29–61
- Qian H (1990) On the statistics of fluorescence correlation spectroscopy. *Biophysical Chemistry* 38:49–57
- Qian H, Elson EL (1990a) On the analysis of high order moments of fluorescence fluctuations. *Biophys J* 57:375–380
- Qian H, Elson EL (1990b) Distribution of molecular aggregation by analysis of fluctuation moments. *Proc Natl Acad Sci USA* 87:5479–5483
- Rigler R, Mets Ü, Widengren J, Kask P (1993) Fluorescence correlation spectroscopy with high count rate and low background: analysis of translational motion. *Eur Biophys J* 22:169–175
- Saleh B (1978) *Photoelectron Statistics*, Springer, Berlin, p 74